Proceedings of The National Conference
On Undergraduate Research (NCUR) 2017
University of Memphis, TN
Memphis Tennessee
April 6-8, 2017

Simulation And Cycle Analyses For High Bypass Turbofan Engine – A Comparative Study

Christopher Roper, Alain Santos, Skyler Bagely
Department of Mechanical Engineering
Kennesaw State University
Marietta, Georgia 30060

Faculty Advisor: Dr. Adeel Khalid

Abstract

The study includes comparison of low bypass ratio turbo fan engine analytical performance and experimental engine test bench results. Variations in variables such as altitude, throttle setting, and freestream velocity are explored and their effect on the engine performance at various stages is analyzed to determine thrust force, thermal efficiency, propulsion efficiency and total efficiency.

Keywords: Gas Turbine Engine, Parametric Cycle Analysis, Performance Curves

1. Background and Introduction

This research involves conducting a comparison of a high-bypass ratio turbo fan engine simulated on a test bench and parametric cycle analysis of the same engine. The results from these methods of data collection are used to analyze correlation between the two methods of performing turbine engine cycle analysis. Test bench data is acquired using the Price Induction® engine test bench and is verified with the analytical parametric cycle analysis to calculate the thrust and efficiency. The purpose of this research is to gather data on gas turbofan engines from the Price Induction test bench (simulation) and compute the corresponding parameters of the turbofan engine analytically. The test bench uses varying environmental conditions that can be used to collect engine performance data from the simulator. Some of the data collected from the simulator are thrust, efficiency, and pressures/temperatures at specific components in the turbofan engine. Computer Aided Design (CAD) models are generated using SolidWorks. As part of this on-going research, the team performed CFD analyses at the component level of the turbofan engine. The analytical aspect of this research includes solving a combination of equations that compute specific parameters for different parts of the engine at different flight conditions with the ultimate goal of computing the overall thrust and efficiency. The gas turbofan engine that is used in the Price Induction Test Bench is the DGEN 380 engine. This engine is designed for small private aircraft.

The DGEN 380 is a small, lightweight, turbofan engine designed for applications in emerging personal light jet flight. Price Induction is developing this engine to compete in traditional turboshaft propulsion altitudes regimes by maintaining low fuel consumption and noise level [2]. The turbofan engine has five main components that work together. The five components that are analyzed include the fan, compressor, combustion chamber, turbine, and nozzle [6].

As shown in Figure 1, the freestream air intake enters the inlet and makes direct contact with the fan. The fan helps divert majority of the air through the bypass system and the remaining through the core of the engine. Air is then compressed through a series of compressor blades in which the area decreases to increase pressure ratio. With increased pressure, the air enters the burner (a.k.a. combustion chamber), and is mixed with jet fuel [3]. The chemical reaction at high pressure results in the generation of high energy. The high-energy fluid then turns the high and low-pressure turbines to provide power back to the compressor thus completing the propulsion engine cycle. After the extraction of energy, the remainder of fluid is directed to the nozzle to mix with the bypass stream to generate thrust

force. The force body diagram shown in Figure 1. High By-pass engine dynamics depicts the balance of forces that engine designers take into consideration in order to maximize propulsive performance.

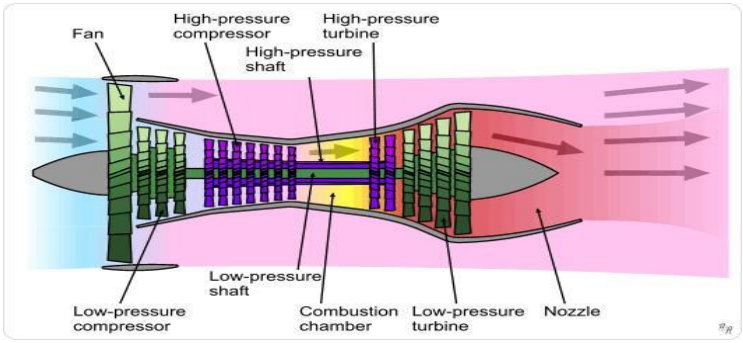

Figure 1. High By-pass engine dynamics

2. Design Specifications and Alternatives

Figure 2 displays the concept design of an ideal Price Induction 4-5 light sport aircraft [1]. The aircraft is designed to be optimum for a cruise altitude of 10,000ft and Mach number of 0.35 with a service ceiling at 25,000ft [8].

Figure 2. GP Aerospace -210 concept design

The DGEN 380 is one of the world's smallest and quietest engines [1]. It produces minimal sound at a range of 255daN output force. The jet has a rated maximum takeoff weight range from 1650 to 2150kg depending on flight conditions [8]. It has an overall height and width of 1346mm and 511mm respectively shown with all other dimension analysis in Figure 3. The Price Induction Test Bench simulates the DGEN 380 engine at various flight conditions.

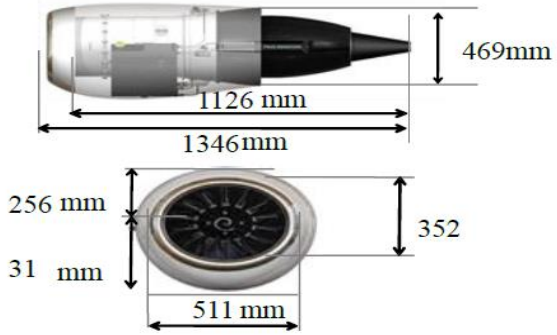

Figure 3. Price Induction DGEN 380 Engine Dimension and Parameters

Figures 4 through 6 show the computer aided models created in SolidWorks. Each major and driving component is modeled in order to recreate accurate dimensions of the DGEN 380. Figure 4 shows the Fan model and half-sectional nacelle.

Figure 4. DGEN 380 prototype fan (left) and bi-sectional nacelle (right) in Solidworks

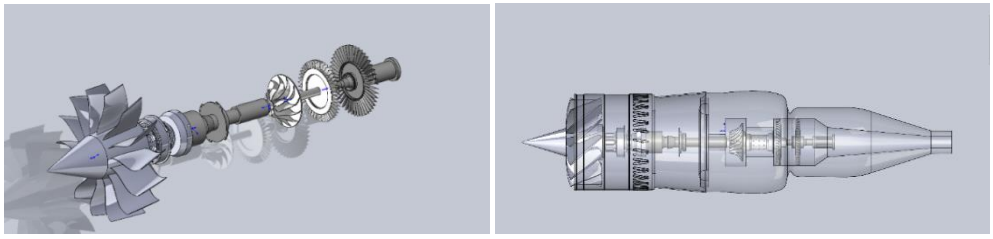

Figure 5. DGEN 380 assembled engine components (left) and components with nacelle cover (right)

Figure 5 represents the assembled fan, centrifugal compressor, low-pressure turbine, and high- pressure turbine components on the left while the right shows the assembled components with the nacelle. Figure 6 shows isometric views of the assembled designed engine of the DGEN 380 in a hidden component view.

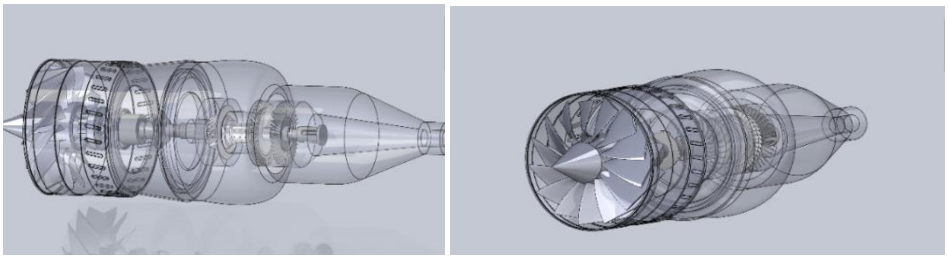

Figure 6. DGEN 380 assembled engine components (left) and components with nacelle cover (right)

3. Methodology

The theoretical analysis is performed using the three propulsion equations to calculate the desired variables as discussed in the Theoretical Analysis section. The DGEN 380 Engine test bench, shown in Figure 7, is used to simulate the engine operation and generate the desired variables. Then experimental data collection and analytical computation, results are plotted. These plots show characteristic relationships of all variables studied. The experimental DGEN 380 engine data is collected at multiple stations shown in Figure 8.

Figure 7. Price Induction Experimental Test Bench

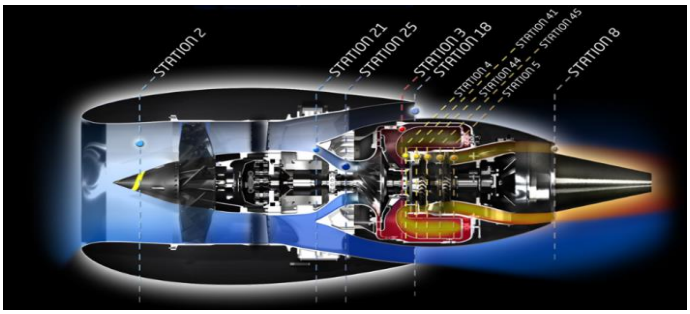

Figure 8. High Bypass Turbofan Engine Station Schematic Dynamics

4. Experimental Analysis

One variable is changed at a time while keeping all the other flight conditions constants in order to determine the optimal operating flight condition for maximum thrust and efficiency. The variables that are explored with Thrust Force output are Power Level Angle (PLA) (otherwise known as throttle setting), Speed, Temperature, and Altitude. Thrust Force and efficiency are computed for each input variable while the other input variables are held constant at their corresponding median values. The median value for input variables are as follows: Speed at Mach 0.22, Temperature: -22.75 (°C), Altitude: 3500 m, and PLA: 50%.

The bench calculates the engine performance for the corresponding control inputs / flight conditions. One variable is changed at a time. Engine performance data are collected by changing each variable one at a time. These data are recorded to generate performance curves. Thrust and Efficiency versus Altitude are calculated while temperature and PLA remain at their median values. Figure 9 depicts the Thrust versus Altitude at various PLA settings. The figure show that as altitude increases, thrust decreases. With 100% PLA, it provides the highest thrust and at 0% PLA, it will be the most efficient.

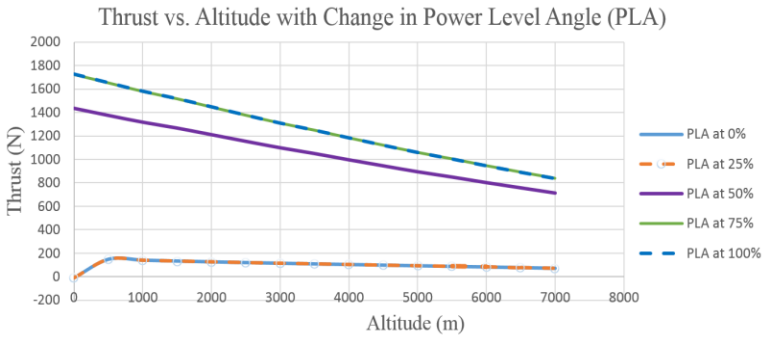

Figure 9. Experimental Thrust versus Altitude with varying PLA%.

Figures 10 shows Thrust versus Altitude at various Mach numbers. As altitude increases, thrust decreases because of the decrease in the density of air directly correlated to the increase in altitude. Thrust versus Altitude with change in

outside temperature shows interesting values referenced in Figure 11. In Figure 11, thrust decreases linearly with altitude with having the best overall characteristic at -0.5°C. The effect of outside air temperature on thrust seems to be less prominent than other control variables.

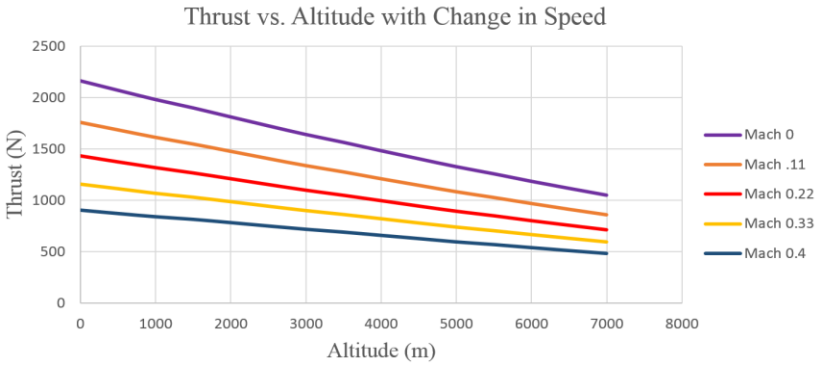

Figure 10. Experimental Thrust versus Altitude with varying Speed.

Thrust versus altitude is analyzed with varying temperatures while keeping the other parameters at their median values. Figures 11 display Thrust versus Altitude with change in Outside Air Temperature. Temperature displays a linear decrease in slope for the overall output for thrust.

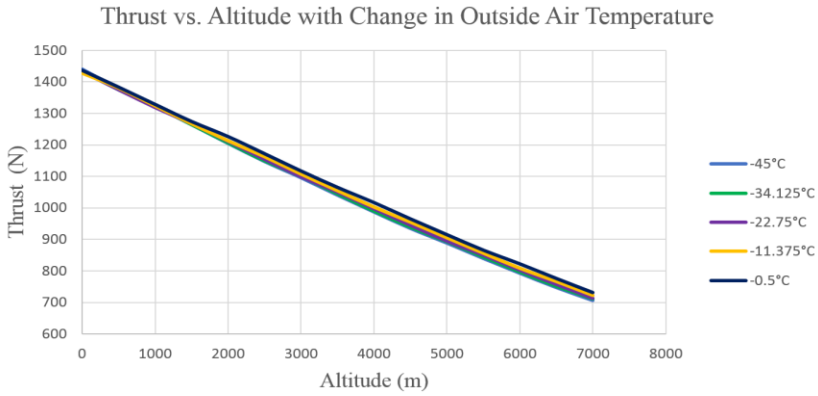

Figure 11. Experimental Thrust versus Altitude with varying Outside Air Temperature.

5. Theoretical Analysis

The Theoretical Analysis is the second method that is explored with parametric analytical equations. The general thrust equation derived from Newton's Second Law can be seen in equation 1. The Turbofan Thrust shows the difference in mass flow rate and velocity is equivalent to thrust force. The simple concept equation relationship is the baseline and foundation for the analytical equations.

$$F = \dot{m}_e V_e - \dot{m}_o V_o + bpr\dot{m}_c V_f \tag{1}$$

$$\frac{F}{\dot{m}_0} = \frac{1}{1+\alpha}\frac{a_0}{g_c}\left[(1+f)\frac{V_9}{a_0} - M_0 + (1+f)\frac{R_t T_9/T_0}{R_c V_9/a_0}\frac{1-P_0/P_9}{\gamma_c}\right] + \frac{1}{1+\alpha}\frac{a_0}{g_c}\left[\frac{V_{19}}{a_0} - M_0 + \frac{T_{19}/T_0}{V_{19}/a_0}\frac{1-P_0/P_{19}}{\gamma_c}\right] \tag{2}$$

$$\eta_T = \frac{a_0^2[(1+f)(V_9/a_0)^2+\alpha(V_{19}/a_0)^2-(1+\alpha)M_0^2]}{2g_c f h_{pr}} \quad (3)$$

$$\eta_P = \frac{2M_0[(1+f)(V_9/a_0)+\alpha(V_{19}/a_0)-(1+\alpha)M_0]}{[(1+f)(V_9/a_0)^2+\alpha(V_{19}/a_0)^2-(1+\alpha)M_0^2]} \quad (4)$$

Various equations are programmed and analyzed using spreadsheets. These mathematical equations help calculate Specific Thrust, Thermal Efficiency, and Propulsive Efficiency analytically. Specific thrust, represented by Equation 2, measures the amount of force per unit mass flow rate. Shown in Equation 3, Thermal efficiency is calculated by taking a ratio of work done by the engine to the heat supplied by the engine. Displayed in Equation 4, is overall propulsive efficiency.

α	bypass ratio	$\dot{m}_e$	engine exit mass flow rate	R_t	Gas constant of turbine
a_o	Free stream speed of sound	M_0	Free stream Mach number	T_0	Free stream temperature
f	Fuel to air ratio	η_p	Propulsive Efficiency	$T_9 = T_8$	Temperature at station 8
F	Uninstalled Thrust	η_t	Thermal efficiency	$T_{19} = T_{18}$	Temperature at station 18
g_c	1	P_0	Free stream pressure	V_0	Free stream velocity
h_{pr}	Low heating value of fuel	$P_9 = P_8$	Pressure at station 8	V_e	engine exit gas velocity
$\dot{m}_0$	Free stream mass flow rate	$P_{19} = P_{18}$	Pressure at station 18	$V_9 = V_8$	Velocity at station 8
$\dot{m}_c$	mass flow rate of the core stream	R_c	Gas constant of Compressor	$V_{19} = V_{18}$	Velocity at station 18
γ_c	Ratio of specific heats at compressor				

At various flight conditions, the control variables are changed one variable at a time and then above equations are used to determine thrust force and overall efficiency. Once calculated the results are then compared and validated with the experimental analysis. Future work includes adding computational fluid dynamic analysis at the component level.

6. Computational Fluid Dynamics

The engine test bench has the ability to simulate thermal and fluid physics and dynamics. Figure 12 shows a visual representation of the fluid physics model. Figure 13 depicts the CATIA v5 baseline models housed in the engine test bench.

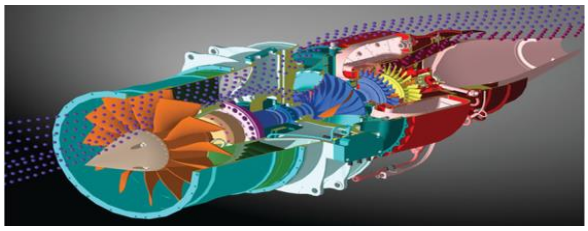

Figure 12. Experimental Computational Fluid Dynamic

Analysis of DGEN 380 Engine

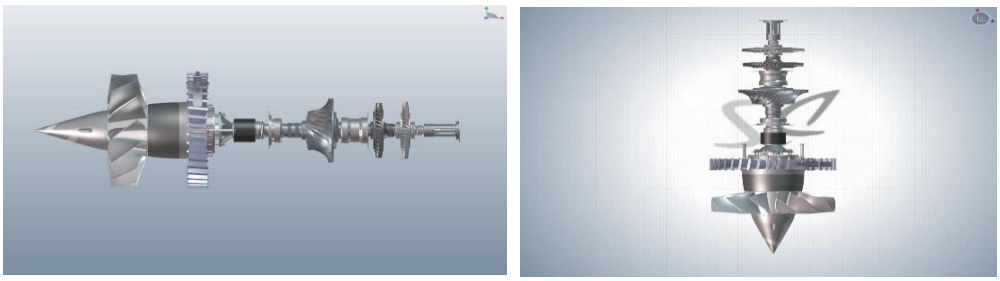

Figure 13. Fan blade model with assembled aircraft engine components in CATIA V5

Using SolidWorks, Computational Fluid Dynamic (CFD) analysis is being performed. CFD will be used to visualize and validate the experimental and theoretical findings for the DGEN 380 turbofan engine. In Figure 14 shows an example of the flow visualization and velocity variation at different parts of the engine.

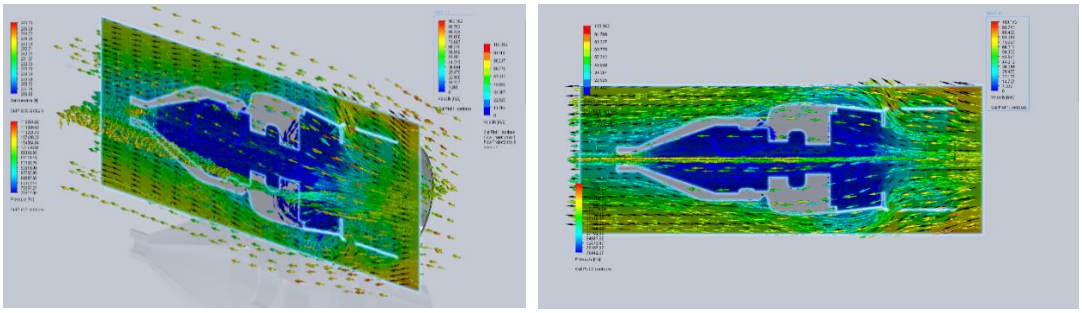

Figure 14. Computational Fluid Dynamic Analysis of Engine Bypass System

The shape of the bypass system and nacelle show that the DGEN 380 has a high bypass ratio. Fluid can be seen traveling at high speeds and proceeding through the system as shown in Figure 17. The data analysis shows that the centrifugal compressor increases the pressure before the combustion chamber. The temperature increases significantly after the mixture of jet fuel and ignition. The chemical kinetics help increase the amount of energy which is then extracted by both the low and high-pressure turbines [10]. The turbines drive the compressor and remaining fluids proceeds through the exhaust to provide thrust force. This helps show the fluid motion interaction with the bypass system as it travels through its projected pathway.

7. Results and Discussion

The intersections of cross points are studied to explore the most optimal and efficient flight conditions. Analytical and experimental analyses are compared. The theoretical calculations displayed in Figures 15 through 20 displays an analytical and experimental comparison analysis for Thrust versus Altitude with varying Mach number, PLA, and Temperature. The analytical approach uses parametric cycle analysis, a methodology in which imperial equations are utilized in real engine performance calculations. Figure 15 represents Thrust vs. Altitude with varying Mach number. The data depicts each set with the same color, calculated and experimental, with its corresponding Mach speed. Thrust and altitude have an inversely proportional relationship. As altitude is increased at each represented speed, output thrust force decreases. The experimental data shows a more dramatic decrease in slope when compared to the analytically calculated thrust. The analytical approach shows an ideal baseline result whereas experimentally, there are more natural environmental factors that are not considered in the parametric cycle analysis calculations. Figure 19 shows Efficiency versus Altitude with varying Mach numbers. The Thrust relationship in directly proportional to altitude. As altitude increases, the overall efficiency increases respectively. This trend can be explained by breaking the overall Efficiency into its two constituents, propulsive and thermal efficiency. Taking a closer look at the two efficiencies, it can be seen that at any flight Mach number the propulsive efficiency decreases a small amount (approximately 0.2 % per 500m increase in altitude). This is because the air is less dense at higher altitudes and leads to a lower fuel to air ratio as well as a smaller thrust force produced by the engine exhaust gases and results in lower

efficiency. Next, analyzing the thermal efficiency, it can be seen that efficiency increases as the altitude increases (approximately 1% per 500m). This increase in thermal efficiency is due to the fact that air breathing jet turbine engines are more efficient when the inlet temperature is colder. When these two values are multiplied together to make overall efficiency the decrease of the propulsive is less than that of the thermal efficiency and leads to an overall increase in overall efficiency.

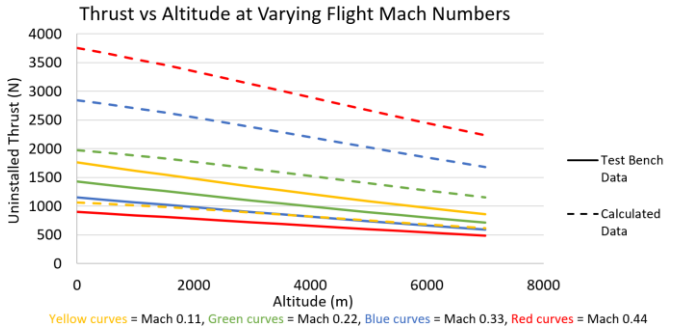

Figure 25. Thrust vs. Altitude with varying Mach number speeds. A theoretical and experimental comparison analysis.

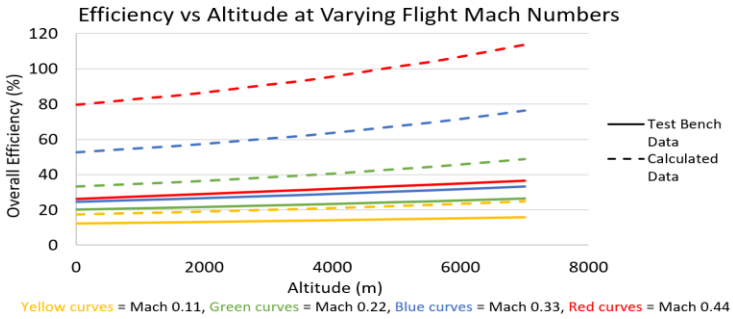

Figure 16. Efficiency vs. Altitude with varying Mach numbers.

Figure 17 displays Thrust versus Altitude with change in PLA%, in which the relationship is inversely proportional. As altitude increases with constant power level angle setting, thrust force will decrease linearly. Due to altitude increase, the air molecules become less dense and it more difficult to combust. Therefore, the amount of fuel burned due to PLA is required to be higher to compensate the low fuel to air ratio at high altitudes. In Figure 18 shows Efficiency versus Altitude with change in PLA%. It shows a directly proportional relationship. As altitude increases, efficiency increases at varying PLA% respectively. At a 50% PLA, it provides the balanced amount of fuel to provide the combustor to atomized fuel molecules. When atomized, each molecule has the ability to ignite and causes a change reaction. If too much PLA% is applied, not all fuel can become atomized. If too little is applied, there will not be sufficient fuel to combust with air. As shown in Figure 17 and 18, the theoretical calculated results show the similar trends as the experimental results and at a number of flight conditions match closely. For other flight conditions, it is expected that the rest bench results are of a higher fidelity than the analytical results. This can be attributed to factors like linearization of analytical equations and non-uniform changes in density as a function of altitude.

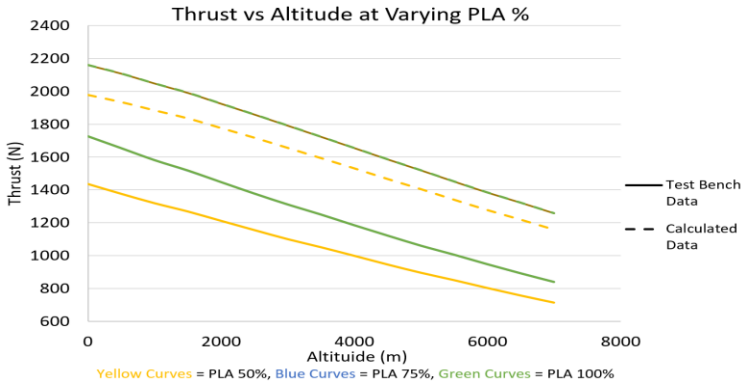

Figure 17. Thrust vs. Altitude with change in PLA %. A theoretical and experimental comparison analysis

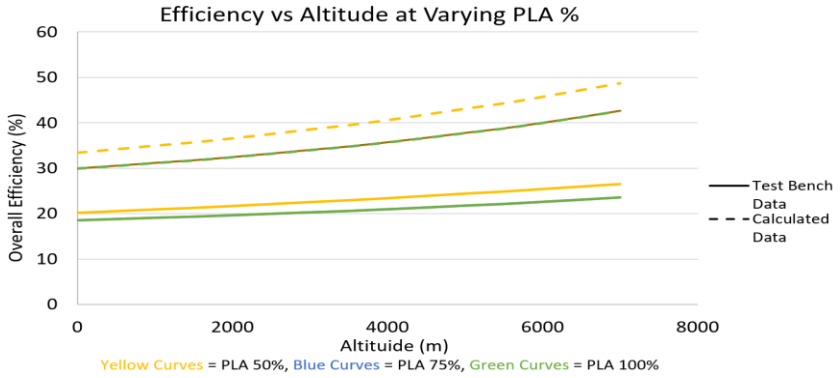

Figure 18**.** Efficiency vs. Altitude with varying PLA % values. A theoretical and experimental comparison analysis.

Figure 19 and 20 shows the comparison of the Thrust and Efficiency versus Altitude with change in Temperature values respectively. As altitude increases with each temperature set, the thrust force decrease at lower environmental temperatures, the air is denser and makes the compression and combustion process more efficient. Higher temperatures increases the kinetic energy within air molecules, when compressed and combusted, the energy output will have less efficient extraction out of the turbines. In result, Figure 20 depicts the directly proportional relationship of Efficiency, as temperature increases the efficiency also increases. The analytical and experimental results show similar trends.

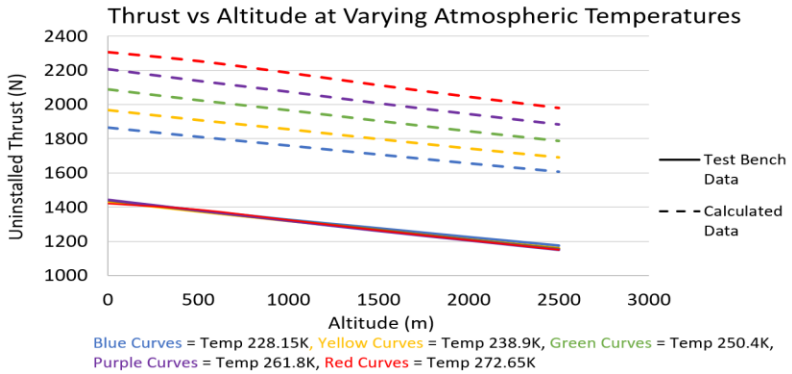

Figure 19. Thrust vs. Altitude with varying Temperature. A theoretical and experimental comparison analysis.

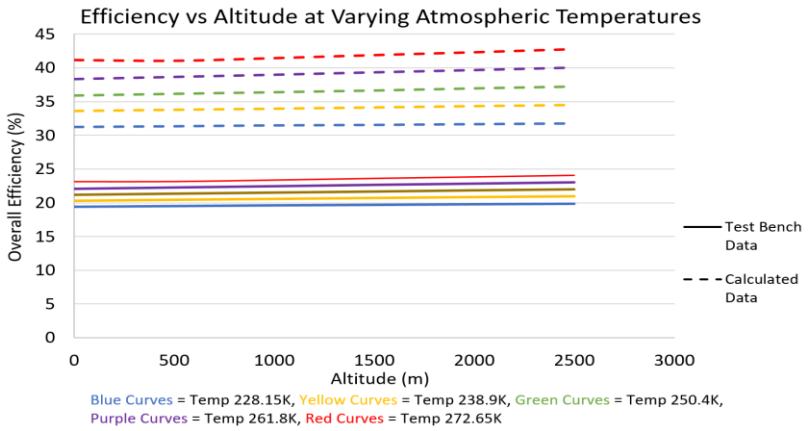

Figure 20. Efficiency vs. Altitude with varying Temperature. A theoretical and experimental comparison analysis

8. Conclusion

The DGEN 380 Engine test bench is to replicate the experimental simulation of propulsive dynamics and generates the desired variables. From experimental and analytical data collection, graphical and plotted recordings of performance curves show a characteristic relationship of all variables. Parametric cycle analysis is used to analytically calculate the thrust and efficiency values. The intersections of cross points are studied to explore the most optimal and efficient flight conditions. Thrust and efficiency are calculated by changing one variable at a time. The design variables include outside air temperature, altitude, Mach number and PLA. While one variable is changed, others are kept constant at their median values. Plots are generated to compare the results obtained from the two different methods. It is observed that the results of the two methods correlate well at various flight conditions. At other flight conditions, they show similar trends but show certain level of discrepancy.

An analysis trade study between the theoretical and experimental testing is validated by using computer aid design package software from computational fluid dynamic analysis. Computer aid design software packages helps visually and experimentally analyze fluid and dynamic forces The thrust force on varied components of the engine stages is analyzed to determine the overall propulsion thrust force. Thus, a comparison study amongst all three methods of experiments is validated through demonstration. The results are expected to match Price Inductions published values; the theoretical analysis, overall output thrust force, and specific fuel consumption is validated through this aircraft experimental propulsion research. This experimentation is a foundation to explore future work with many additional aerodynamic design parameters.

9. Acknowledgements

We are highly thankful and appreciative to our faculty advisor Dr. Adeel Khalid for his active guidance throughout the completion of the research project. Extensions of our appreciation as serves to Skyler Bagley for prior research participation and data collection.

10. References

1. Berton, Jeffrey J. “System Noise Prediction of the DGEN 380 Turbofan Engine.” NASA. NASA, 30 Sept. 2015. Web. 28 Jan. 2017.

2. Keith, Jr. A.L. “A Brief Study of the Effects of Turbofan-Engine Bypass Ratio on Short-Long-Haul Cruise Aircraft.” A Brief Study of the Effects of Turbofan-engine Bypass Ratio on Short-and Hong-haul Cruise Aircraft (n.d.): n.pag.Nrts.nasa.gov. Dec. 1975. Web.

3. Liu, F., and W. A. Sirignano. "Turbojet and Turbofan Engine Performance Increases Through Turbine Burners." Vol. 17, No. 3, May – June 2001 Turbojet and Turbofan Engine Performance Increases Through Turbine Burners (n.d.): n. pag. Http://fliu.eng.uci.edu/Publications. May-June 2001. Web.

4. Takikame, Carlos Eduardo Takikame. Control and Management of Motor Aeronautical Fadec. Tech. no. ISSN 2179-7625. 6th ed. Vol. 5. Taubaté: n.p., 2014. Print. Ser. 3.

5. Kestner, Brian K., Jeff S. Schutte, Jonathan C. Gladin, and Dimitri N. Mavris.ULTRA High Bypass Ratio Engine Engine Sizing and Cycle Selection Study for a Subsonic Commercial Aircraft in the N+2 Timeframe. Tech. no. GT2011-453. Vancouver: ASME, Canada. Print.

6. Vogeler, Konrad. The Potential of Sequential Combustion For High Bypass Jet Engines. Tech. no. 98-GT-311. THE AMERICAN SOCIETY OF MECHANICAL ENGINEERS, June 1998. Web.

7. Elfarral, Monier A., Nilay Sezer Uzol, and Sinan Akmandor NREL VI Rotor Blade: Numerical Investiagion and Winglet Design and Optimization Using CFD. Tech Journal of Fluids Engineering 2002; 124: 393-399.

8. "Price Inductions." Turbine Technologies, n.d. Web. 31 July 2015.

9. “Wind Map | NOAA Climate.gov.” Wind Map | NOAA Climate.gov. National Centers for Environmental Information, n.d, Web. 25 July 2015.

10. Francesco Balduzzia, Alessandro Bianchinia, Riccardo Malecia, Giovanni Ferraraa, Lorenzo Ferrarib, ‘Critical issues in the CFD simulation of Darrieus wind turbines,’ Renewable Energy, Volume 85, January 2016, Pages 419–43 [11] Abdullah Mobin Chowdhurya, Hiromichi Akimotoa, Yutaka Harab, ‘Comparative CFD analysis of Vertical Axis Wind Turbine in upright and tilted configuration,’ Renewable Energy, Volume 85, January 2016, Pages 327–337